




Concordance Analysis of Microsatellite Instability via NGS and Mismatch Repair Deficiency via IHC in Endometrial and Colorectal Cancer

Camilla Nero^{1,2} · Lisa Salvatore^{2,3} · Simona Duranti⁴ · Gloria Anderson^{1,2}  · Luca Mastrantoni² · Mina Karimi⁵ · Giulia Mantini⁵ · Angelo Minucci⁶ · Giulia Maneri⁶ · Luciano Giacobbe⁵ · Angela Santoro⁷ · Arianna Panfili⁴ · Alessia Piermattei⁷ · Ilenia Marino⁴ · Giulia Caira³ · Maria Alessandra Calegari³ · Giovanni Trovato³ · Valentina Iacobelli^{1,2} · Vanda Salutarì¹ · Nicola Normanno⁸ · Francesco Fanfani^{1,2} · Giovanni Scambia^{1,2} · Giampaolo Tortora^{2,3}

Received: 6 October 2025 / Accepted: 13 January 2026 / Published online: 25 February 2026
© The Author(s) 2026

Abstract

Background Assessment of mismatch repair (MMR) function provides critical guidance for diagnosis, prognosis, and therapeutic decision making in colorectal and endometrial cancers. Mismatch repair immunohistochemistry (IHC) is the routine clinical test for identifying MMR deficiency, while microsatellite instability (MSI) serves as its surrogate, detected by polymerase chain reaction or next-generation sequencing (NGS). Available data indicate a high concordance rate between these approaches in colon cancer, whereas a lower concordance has been reported in endometrial cancer.

Objective We aimed to assess the concordance rate between MMR-IHC and MSI-NGS from patients with colorectal or endometrial cancer, using IHC as the gold standard.

Methods A cohort of 520 patients (352 with endometrial cancer and 168 with colorectal cancer) were included. MMR-IHC assessed MLH1, MSH2, MSH6, and PMS2 expression, while MSI-NGS was determined by profiling 130 homopolymer repeat loci using the TruSight Oncology 500 panel from Illumina.

Results While concordance was high in the colorectal cancer cohort (99%, 95% confidence interval 96–100), a lower level of agreement was observed in endometrial cancer cases (85%, 95% confidence interval 81–89). Fifty-two of 53 discordant cases exhibited MMR deficiency by IHC in the absence of detectable MSI. Forty percent of discordant cases could be explained by factors previously associated with reduced MSI levels, including mutations in DNA polymerase genes ($n = 5$), isolated MSH6 loss ($n = 10$), atypical IHC staining patterns ($n = 8$), and germline variants ($n = 6$). Additionally, the presence of genetic and epigenetic alterations (specifically, 19 cases with MLH1 promoter hypermethylation and ten with somatic or germline MMR variants) supports the interpretation that MSI calls were missed in a subset of cases. Finally, optimizing the MSI threshold enhanced detection accuracy in endometrial tumors.

Conclusions These findings confirm the lower concordance between MMR-IHC and MSI-NGS in endometrial cancer compared with colorectal cancer when broad panels are used, underscoring the importance of tumor-specific interpretation even within tumor-agnostic assays. Although cut-off optimization improved agreement, the evidence remains insufficient for clinical implementation, and further validation studies are needed.

Key Points

The concordance between microsatellite instability-next-generation sequencing and mismatch repair-immunohistochemistry is lower in endometrial cancer than in colorectal cancer.

Most discordant cases show mismatch repair deficiency by immunohistochemistry but remain Microsatellite Stability by next-generation sequencing.

Approximately 40% of discordant cases could be attributable to one or more previously described factors.

Camilla Nero and Lisa Salvatore contributed equally to this work.

Giovanni Scambia and Giampaolo Tortora contributed equally to this work.

1 Introduction

The mismatch repair (MMR) system is a conserved mechanism that preserves genomic integrity, by detecting and repairing DNA errors such as single-base mismatches or short insertions and deletions, involving the proteins MLH1, MSH2, MSH6, and PMS2 [1]. In tumors with MMR deficiency (dMMR), replication errors frequently arise within microsatellites, which are DNA sequences consisting of one to six nucleotide units repeated in tandem, leading to alterations in the length or sequence of these repetitive regions. Mismatch repair deficiency in tumors is mostly (60–80%) caused by *MLH1* gene promoter hypermethylation or somatic bi-allelic mutation in *MMR* genes [2–5]. Less commonly (10–30% of dMMR) [6], it arises from an autosomal dominant heterozygous germline variant of *MMR* genes, delineating Lynch syndrome, which increases the risk of cancer, particularly colorectal cancer (CRC) and endometrial cancer (EC).

Integrated genomics data from The Cancer Genome Atlas Network show that around 12% of CRC samples and 30% of EC samples exhibit MSI-high (MSI-H) with a hypermutated phenotype [7, 8]. This feature is linked to prognosis and response to immunotherapy in both cancer types [9, 10]. In CRC, dMMR is commonly linked to right-sided colon involvement, a mucinous phenotype, tumor-infiltrating lymphocytes, a Crohn's-like inflammatory reaction, multiple tumor subclones, and poor differentiation, and frequently co-occurs with *BRAF* mutations [11]. In non-metastatic CRC, dMMR correlates with a good prognosis and limited benefit from adjuvant therapy, particularly fluoropyrimidine [12]. In metastatic CRC, though rare (1–2%), dMMR indicates a poor prognosis, a reduced response to standard chemotherapy, and a significant benefit from immune checkpoint inhibitors [13], such as ipilimumab with nivolumab and pembrolizumab. In EC, dMMR is associated with endometrioid histology, an intermediate prognosis [14], and this subgroup benefits significantly from immune checkpoint inhibitors [15–17]. Approved immune checkpoint inhibitors for advanced or metastatic dMMR EC include pembrolizumab and dostarlimab as monotherapies, as well as combined with platinum-based chemotherapy [15–17]. Additionally, pembrolizumab is approved in combination with lenvatinib for advanced or recurrent EC after prior platinum-based therapy [18].

For both predictive and prognostic purposes, as well as for Lynch syndrome screening, assessing MMR function in all patients with newly diagnosed CRC and EC is strongly recommended by international and national guidelines [19]. Immunohistochemistry (IHC) for MMR proteins offers adequate sensitivity and specificity for detecting dMMR [20]. Microsatellite instability testing serves as a proxy for MMR

abnormalities, measuring the consequences of its deficiency through polymerase chain reaction (PCR) or next-generation sequencing (NGS) techniques [21]. Available data indicate a high concordance between these approaches in CRC, in particular between IHC-MMR and PCR-MSI, whereas a substantially lower concordance has been observed in EC (80–100%) [22–30].

Moreover, MMR assessment is not the only molecular feature to be considered in both CRC and EC. The increasing complexity of genomic alterations has prompted referral centers to adopt comprehensive cancer genome profiling [21]. Although these NGS-based assays indicate MSI status, there is limited evidence assessing their accuracy when compared to IHC-MMR and PCR-MSI evaluations. Next-generation sequencing can evaluate thousands of microsatellite loci compared with 5–7 loci detected by PCR [31, 32] and the MSI cut-off in different tumor types is controversial, requiring further clarification.

Thus, the present study aims to evaluate the concordance rate between the NGS-MSI status compared with the gold standard IHC-MMR in an unselected prospective series of CRC and EC patients from a large referral center. Additionally, a detailed genomic, pathological, and clinical analysis of discordant cases was conducted to investigate the underlying causes of the discrepancies.

2 Material and Methods

2.1 Study Population

At Fondazione Policlinico Universitario Agostino Gemelli IRCCS (FPG), patients with specific solid tumors were offered a tumor-only targeted NGS panel as part of an institutional cancer genome profiling program (ClinicalTrials.gov Identifier: NCT06020625, Protocol ID: FPG500). This program follows the Declaration of Helsinki guidelines and received approval from the local ethical committee (Protocol U 00194/23, ID number: 3837). All patients provided informed consent before participation. This study included all consecutive patients with CRC and EC with available IHC-MMR and NGS-MSI evaluations.

2.2 IHC and NGS

Details on the IHC and NGS approach have been previously published and summarized in the Electronic Supplementary Material (ESM) [33–35]. Histopathologic data were obtained from standardized pathology reports (<https://www.mayocliniclabs.com/test-catalog/overview/35466>).

For the NGS analysis, the TruSight Oncology 500 (TSO500) panel (Illumina, San Diego, CA, USA) was used,

targeting 523 genes for substitutions, insertions/deletions, copy number alterations, selected gene rearrangements, and tumor mutational (TMB). Microsatellite instability status was assessed by analyzing 130 homopolymer repeat loci and covered by a minimum of 60 full-spanning reads, with at least 40 loci required for an MSI score. An MSI score above 20% classified patients as MSI-H, per Illumina TSO500HT guidelines [36]. Microsatellite instability status was reported but not used clinically. The SigProfilerAssignment tool was used to compute previously known mutational signatures (COSMIC signatures) [37] and SigProfiler was employed to identify single-base-substitution (SBS) mutational signatures.

2.3 Statistical Analyses

Results were expressed as the median and interquartile ranges (IQRs) or as number and percentages. Diagnostic performance of NGS-MSI in detecting dMMR status was evaluated using IHC-MMR as the gold standard. Sensitivity, specificity, accuracy, positive predictive value, and negative predictive value (NPV), and Cohen's kappa coefficient with 95% confidence interval (CI) were calculated to assess the agreement between IHC-MMR and NGS-MSI. The Mann-Whitney U test was used for comparing medians. Misclassified cases (dMMR/MSS or proficient MMR [pMMR]/MSI-H) were further stratified by TMB into low (<10 mut/MB) or high (\geq 10 mut/MB). No missing values were replaced nor imputed. All statistical analyses were conducted using R Studio, data visualizations were generated using R packages (ComplexHeatmap, Circlize, maftools, ggplot2) [38–41].

3 Results

From January 2022 to May 2023, a cohort of 404 EC and 232 CRC cases was profiled within an institutional cancer genome profiling program. The NGS-MSI and IHC-MMR evaluations were available for 520 patients (352, 86% of patients with EC; 168, 72% of patients with CRC) as shown in Fig. 1.

The overall concordance between NGS-MSI and IHC-MMR was 90% (CI 87–92). Using IHC as the reference standard for dMMR detection, NGS-MSI demonstrated 62% sensitivity and 99% specificity (Fig. 2a).

Positive predictive value was 98% and NPV was 88%. In the EC cohort, concordance was 85% (CI 81–89%), with 59% sensitivity (CI 54–64%) and 99% specificity (CI 98–100%), while the CRC cohort showed 99% concordance (CI 96–100%), with 87% sensitivity (CI 81–91%) and 100% specificity (CI 90–100%) as shown in Fig. 2b and c. The EC cohort reported a positive predictive value of 99% (IC: 96–99%) and NPV of 82% (CI 77–86%), while the CRC cohort had a positive predictive value of 100% (CI

98–100) and NPV of 99% (CI 95–100). Cohen Kappa values were 0.65 (CI 0.56–0.73) for EC and 0.92 (CI 0.81–1) for CRC (both $p < 0.001$). The median MSI score in patients with dMMR EC was 24.42 (IQR: 10–40.67) and 2.44 in pMMR EC (IQR: 1.59–3.75) as shown in Fig. 3. MMR deficiency CRC displayed a median MSI score of 52.85 (IQR: 28.92–64.10; Fig. 1) while 2.48 (IQR: 1.59–4) was found in the pMMR subgroup.

Among the 130 microsatellite loci included for the MSI assessment, only 127 were evaluable. The median value of usable loci was 122 (range 53–127) in CRC cases and 123 (range 51–127) in EC cases, with 127 overlapping usable loci between CRC and EC (Fig. 1 of the ESM). Considering all cases (168 CRC and 352 EC), the majority of patients with EC exhibited instability at three specific loci (18:57571785, 31.2%; 22:29696468, 26.4%; 22:29682881, 22.4%). In CRC, the loci most commonly affected were 7:14028189 (21.4%), 13:28962591 (20.8%), and 18:57571785 (20.2%). When examining the median frequency of instability across all usable loci (8.07%), 62 loci fell below this value. Overall, patients with EC showed significantly more frequent instability events across the 127 loci analyzed than patients with CRC ($p < 0.01$; Fig. 1A of the ESM). When analysis was restricted to MSI-H tumors, however, CRC showed a higher degree of instability ($p < 0.01$; Fig. 1A of the ESM). Moreover, the percentage of unstable loci among patients with EC differed significantly across molecular phenotypes (MLH1/PMS2, MSH2/MSH6, PMS2 only, MSH6 only), with the MSH2/MSH6 subgroup showing the highest values and the PMS2-only subgroup the lowest values ($p < 0.001$, Fig. 4A). Of note, within the MLH1-PMS2 subgroup, all MLH1 hypermethylated patients ($n = 19$) showed MSI scores below the detection threshold (0 vs 54, $p < 0.001$). In contrast, dMMR CRC samples generally exhibited a higher percentage of unstable loci compared with dMMR EC samples, except for two cases within the MSH2/MSH6 subgroup, which represent the discordant samples (Fig. 4B). Compared with pMMR/MSS patients, dMMR/MSI-H patients had higher median TMB values ($p < 0.001$; Table 1 of the ESM) and greater enrichment in indels (EC: 24.68% vs 5.04%, $p < 0.001$; CRC: 19.62% vs 9.16%, $p < 0.001$) as shown in Fig. 2 of the ESM.

3.1 Discordant Cases

Figure 5 and Table 2 of the ESM summarize the main molecular and pathological features of the 53 discordant cases: 51 EC (96%) and 2 CRC (4%). The median number of loci used to calculate the MSI score was nearly identical between discordant and concordant cases (123 vs 122). Both discordant CRC cases were dMMR/MSS; one case

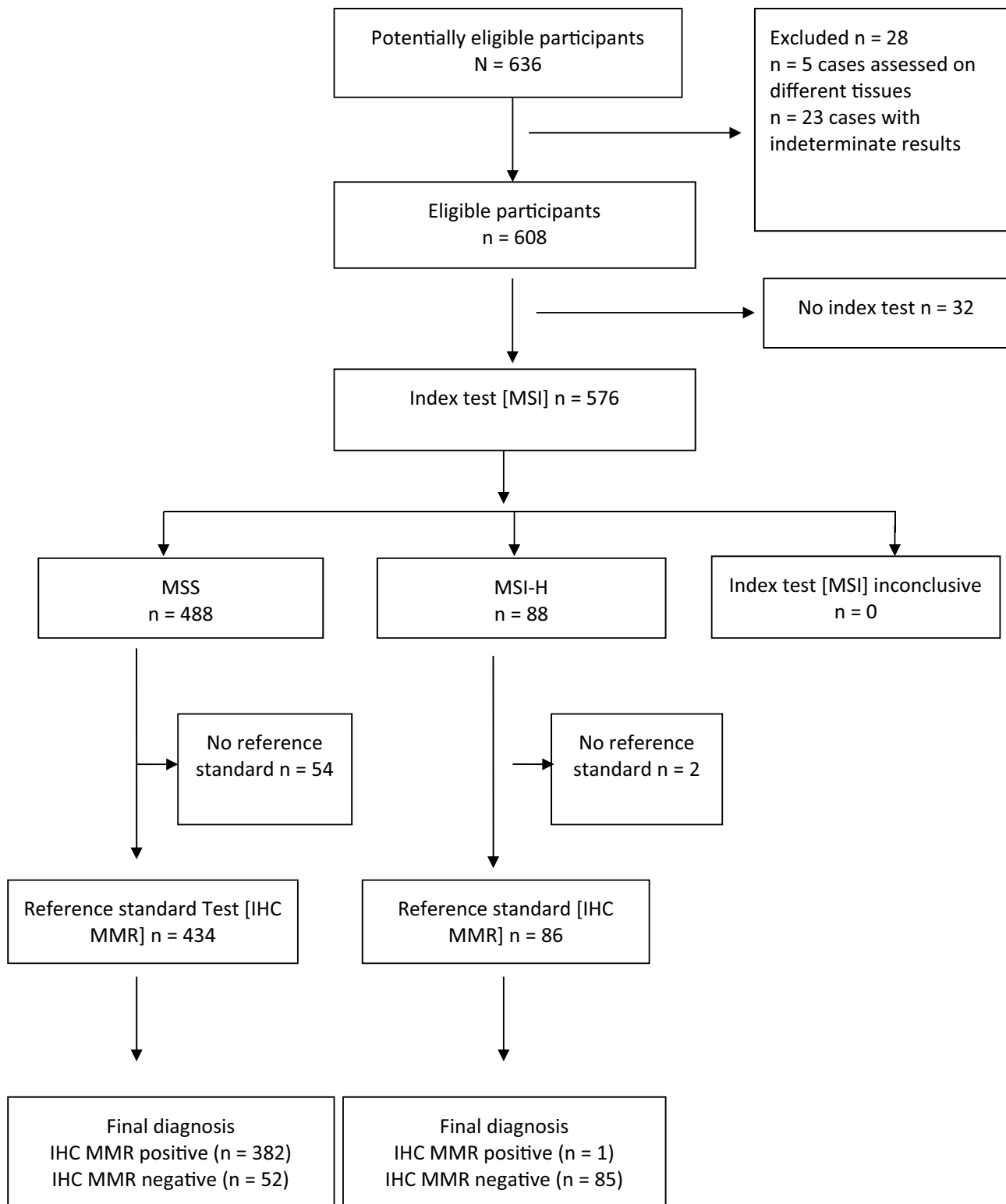


Fig. 1 Standard for Reporting Diagnostic Accuracy (STARD) flow chart. *IHC* immunohistochemistry, *MMR* mismatch repair, *MSI* microsatellite instability, *MSI-H* microsatellite instability-high, *MSS* microsatellite stability

a.

Overall	MMR		Overall
	<i>dMMR</i>	<i>pMMR</i>	
MSI			
<i>MSI-H</i>	85	1	86
<i>MSS</i>	52	382	434
Overall	137	383	520

b.

EC	MMR		Overall
	<i>dMMR</i>	<i>pMMR</i>	
MSI			
<i>MSI-H</i>	72	1	73
<i>MSS</i>	50	229	279
Overall	132	230	352

c.

CCR	MMR		Overall
	<i>dMMR</i>	<i>pMMR</i>	
MSI			
<i>MSI-H</i>	13	0	13
<i>MSS</i>	2	153	155
Overall	15	153	168

Fig. 2 Confusion matrixes for the overall cohort (a), endometrial cancer [EC] (b), and colorectal cancer [CCR] (c). *dMMR* mismatch repair deficiency, *MSI* microsatellite instability, *MSI-H* microsatellite instability-high, *MSS* microsatellite stability, *pMMR* proficient mismatch repair

displayed an atypical IHC-MMR staining pattern. Among the discordant EC cases, 50 were *dMMR/MSS* and one was *pMMR/MSI-H*. In the 50 *dMMR/MSS* discordant EC cases, the most common IHC-MMR alteration was *MLH1/PMS2* loss, occurring in 56% of cases. Additionally, three EC cases involved *MSH2/MSH6* loss, two showed an isolated loss of *PMS2*, and ten (19.6%) exhibited an isolated loss of *MSH6* (Fig. 5).

Five discordant EC cases were classified as *POLE* mutant (*POLEmut*). Their median TMB value was 222 (IQR: 73–380), higher compared with the *dMMR/MSI-H* EC group (33.6 mut/MB; IQR: 21.6–48.7 mut/MB; $p = 0.05$; Tables 1 and 2 of the ESM). At IHC-MMR staining, four cases (*POLE* mutation p.P286R c.857C>G) had a dot-like *MLH1/PMS2* while one case (*POLE* mutation p.S297F c.890C>T) displayed an isolated loss of *MSH6*. *POLE* mutation was considered the driver for concomitant somatic MMR mutations observed in two cases (Fig. 5). All five discordant *POLEmut* cases showed the expected COSMIC signatures (SBS10a, SBS10b), while 20 discordant cases, including 2 *POLEmut*, exhibited the *dMMR*-associated one (see Fig. 3 of the ESM). Atypical patterns of IHC-MMR such as dot-like or partial loss of *MLH1/PMS2* or isolated *MLH1* loss were found in seven *dMMR/MSS* EC.

Compared with the concordant group, discordant EC cases were enriched with *POLE* mutations (9.8% vs 0%, $p < 0.001$) and *MSH6* (19.6% vs 1.68%, $p < 0.01$, Fisher’s exact test). By contrast, the difference in tumor cell content between the two groups did not reach a statistical significance (70 vs 80, $p = 0.07$, Mann–Whitney U test).

Within the *MLH1/PMS2*-altered EC subgroup, the evaluation of *MLH1* hypermethylation was available for 86% of cases; of these, 64% were found to be hypermethylated. In ten cases of *dMMR/MSS* EC, somatic variants in MMR genes were identified; of these, two showed concomitant *POLE* mutations as previously mentioned, while six were confirmed to be of germline origin (three with an isolated deficit of *MSH6* and germline pathogenic variants in *MSH6*).

Excluding *POLEmut* cases, both EC and CRC *dMMR/MSS* cases had significant lower TMB values than *dMMR/MSI-H* cases ($p = 0.04$; Fig. 3). Similarly, the rate of indels in this subgroup was lower than in *dMMR/MSI-H* cases ($p < 0.001$; Fig. 3 of the ESM).

In our cohort, an MSI threshold of 6.1 was identified as optimal for classifying *dMMR* status in EC, achieving an area under the curve of 0.9 (sensitivity = 81%, specificity = 96.5%) [Fig. 4a of the ESM].

This threshold accurately reclassified 26 discordant cases as *dMMR/MSI-H* but incorrectly classified six *pMMR/MSI-H* patients, previously concordant, reducing the overall number of discordant cases to 31. Of the 26 reclassified cases, 12 exhibited *dMMR*-associated COSMIC signatures (Fig. 4 of the ESM). Conversely, the optimal discriminating threshold in CRC cases was 14.97, achieving a sensitivity of 86.7% and a specificity of 100% in patients with CRC (Fig. 4b of the ESM).

Finally, from a therapeutic point of view, ICIs were administered to 13 patients with *dMMR* CRC and two patients with *dMMR* EC. Among CRC cases, the two *dMMR/MSS* patients progressed after 3.3 and 7.1 months,

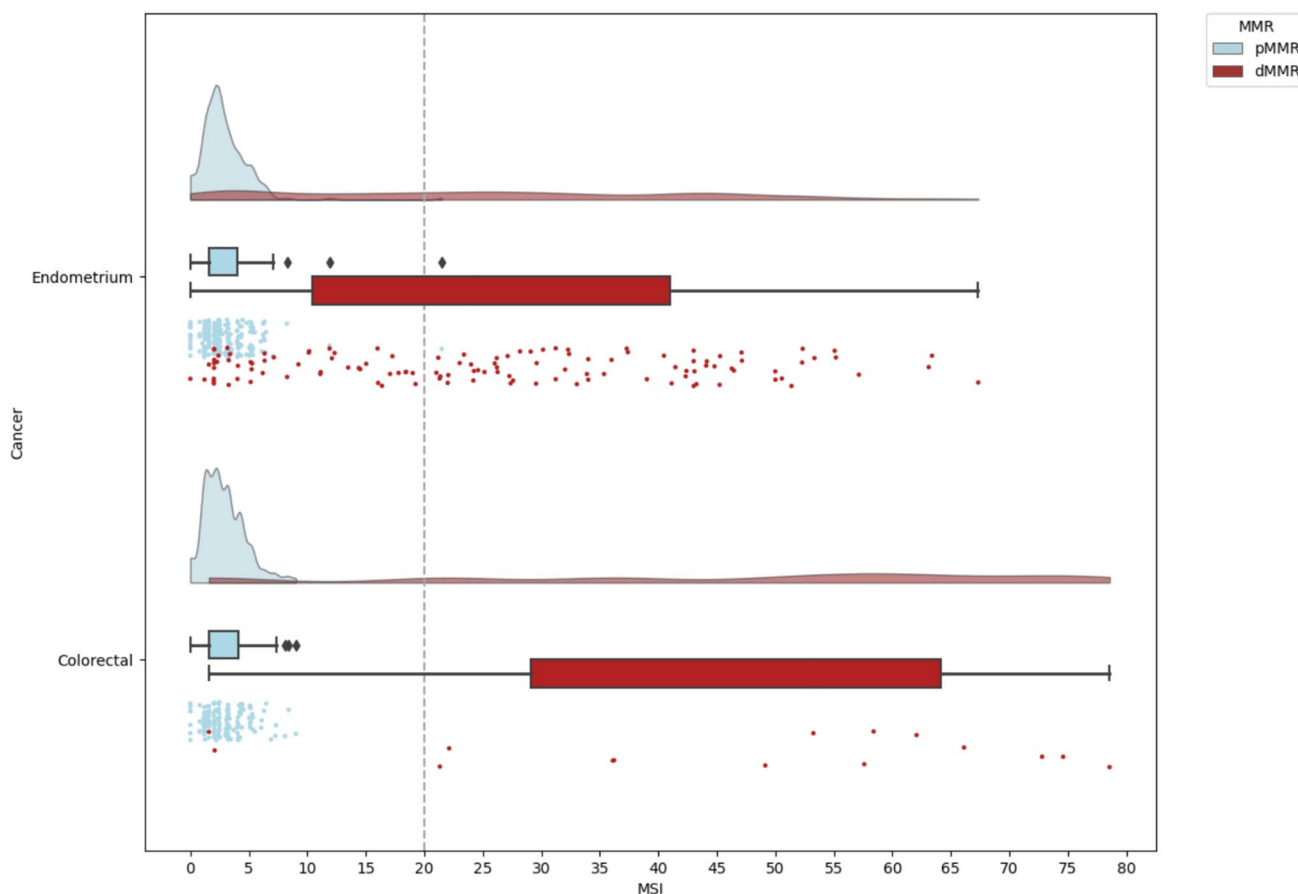


Fig. 3 Raincloud plot of the study cohort divided by patients with endometrial cancer and patients with colorectal cancer. *dMMR* mismatch repair deficiency, *MMR* mismatch repair, *pMMR* proficient mismatch repair

respectively, as shown in Fig. 6. For both patients with *dMMR/MSI-H* EC, ICI treatment is currently ongoing.

4 Discussion

Mismatch repair/MSI status is of substantial clinical importance because of its key role in the diagnostic, prognostic, predictive, and therapeutic stratification of various cancers, particularly EC and CRC, and for universal screening for Lynch syndrome. Our study shows an overall 90% concordance rate between NGS-MSI and IHC-MMR in a large unselected series of prospectively clinically sequenced patients with CRC and EC from a large referral center. This rate was lower in EC cases (85%) compared with CRC cases (99%).

Available evidence has consistently shown a high concordance between MMR-IHC and MSI testing in CRC, particularly when MSI is assessed by PCR, whereas a substantially lower concordance has been reported in EC. In the latter, the concordance rate comparing IHC with an MSI assessment using different methodologies,

including the Bethesda and Promega panels, Idylla™, the amplicon-sequencing-based Newcastle MSI assay, and NGS-based approaches, showed values that ranged from approximately 80% to nearly 100% [22–30]. This difference between diseases can be partially explained by the fact that unstable microsatellite markers in CRCs show significantly larger nucleotide shifts than those in ECs. In contrast, the minimal shifts typical of ECs may be missed, in particular when tumor cellularity is <30% or when PCR signal intensity is low, leading to false-negative MSI results [5, 29, 30].

Two studies have focused specifically on NGS-MSI rather than PCR-MSI. It is important to note that among the microsatellite markers typically present within commonly used PCR-based MSI panels, the assay used in this study includes only the NR21 mononucleotide (locus *SLC7A8*, chr14:23652346).

In a small cohort study (28 CRC, 21 EC) comparing IHC-MMR, PCR-MSI, and NGS-MSI, a lower concordance in EC (94–96%) compared with CRC (99%) was found, regardless of the method [42]. In a large cohort of 1942 solid (CRC, $n = 609$; EC $n = 3$) cancer cases profiled with TSO500 HT,

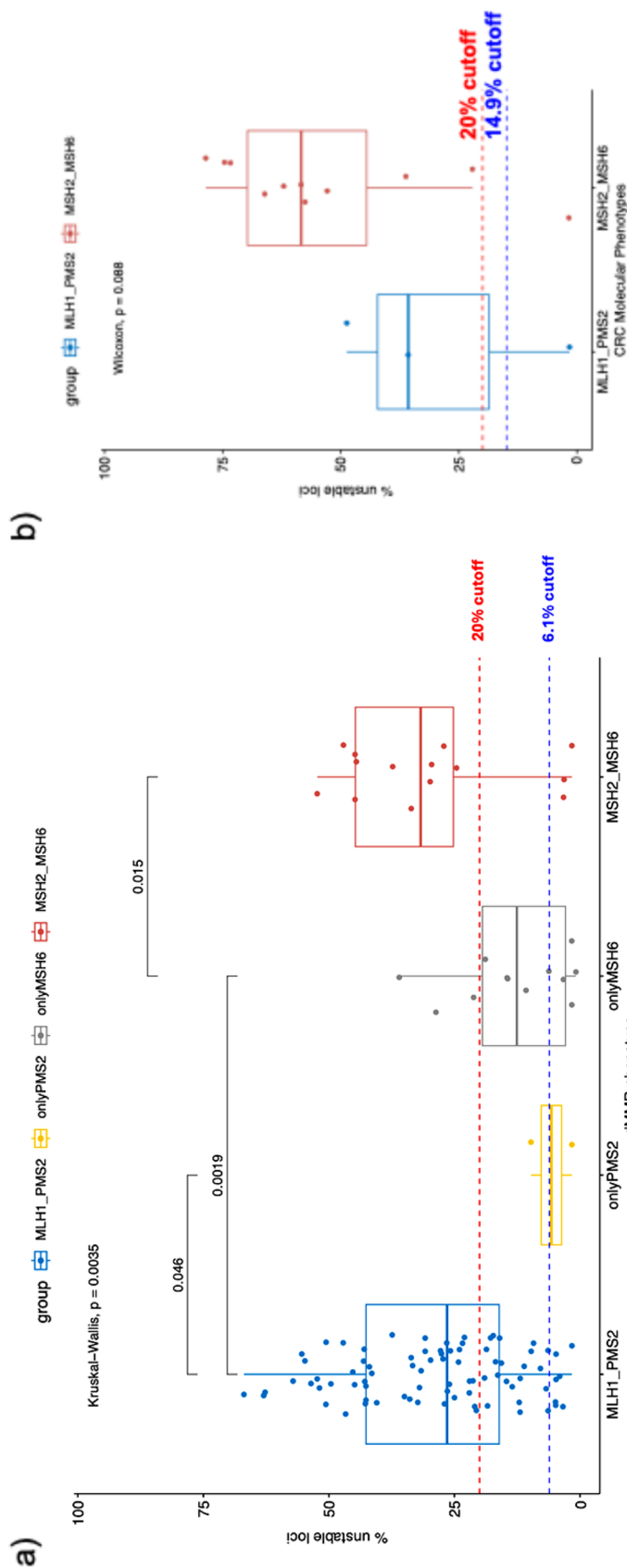


Fig. 4 a) Boxplots for each molecular phenotypes, namely MLH1 and PMS2 (no MLH1 hypermethylated and MLH1 hypermethylated and MSH2 and MSH6, PMS2 only, MSH6 only, MSH2 only, showing the percentage of unstable loci for each mismatch repair deficiency endometrial cancer (EC) sample ($n = 116$). **b)** Boxplots for each colorectal cancer (CRC) mismatch repair deficiency subgroup ($n = 14$) namely MLH1_PMS2 and MSH2_MSH6. Statistics was computed for each group combination and the p -value is shown only for significant differences ($p < 0.05$)

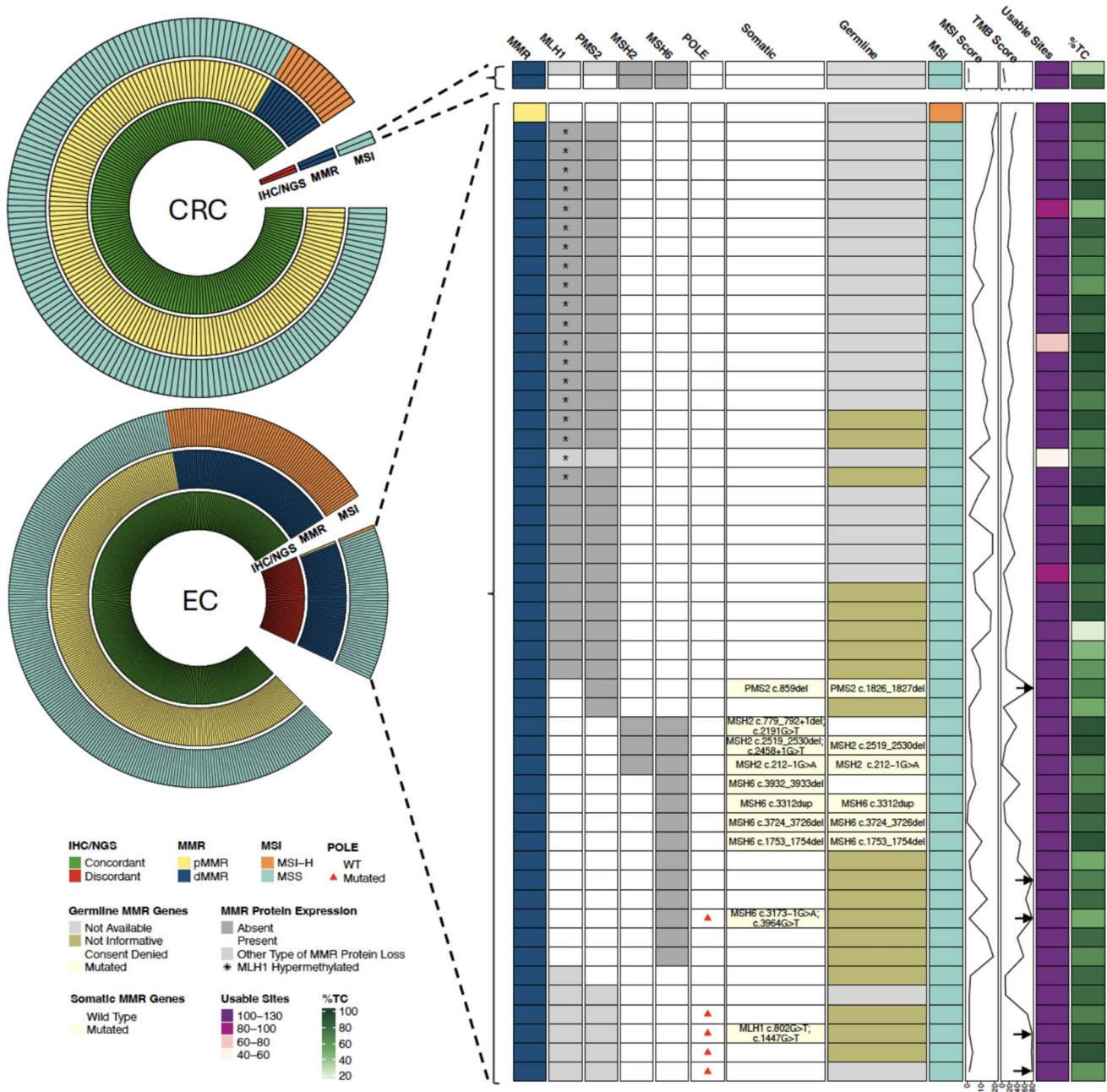


Fig. 5 Characteristic of discordant cases ($n = 53$). *CRC* colorectal cancer, *dMMR* mismatch repair deficiency, *EC* endometrial cancer, *IHC* immunohistochemistry, *MMR* mismatch repair, *MSI* microsatellite instability, *MSI-H* microsatellite instability-high, *MSS* micro-

atellite stability, *NGS* next-generation sequencing, *pMMR* proficient mismatch repair, *TC* tumor cells percentage, *TMB* tumor mutational burden, *WT* wild type

only ten patients were discordant (dMMR/MSS using a cut-off of 20%) [43]; to avoid discrepancies, the authors suggested introducing a borderline MSI category (MSI score ≥ 7 and $< 20\%$) and confirming results with PCR-MSI and IHC-MMR. Similarly, our results indicate that by lowering the MSI score threshold to 6.1, the overall number of discordant cases can be reduced to 31 (sensitivity 81.1%, specificity 96.5%). This is further supported by differences

in the number of unstable loci among MMR phenotypes, likely explaining reduced MSI scores in cases with MLH1/PMS2 loss, which account for 56% of discordant EC cases.

One or more known potential causes of discordance were found in 21 out of 53 discordant cases including *POLE* mutations, isolated MSH6 loss, atypical MMR-IHC staining patterns, germline variants, and low tumor content; the first two were significantly enriched in the discordant subgroup

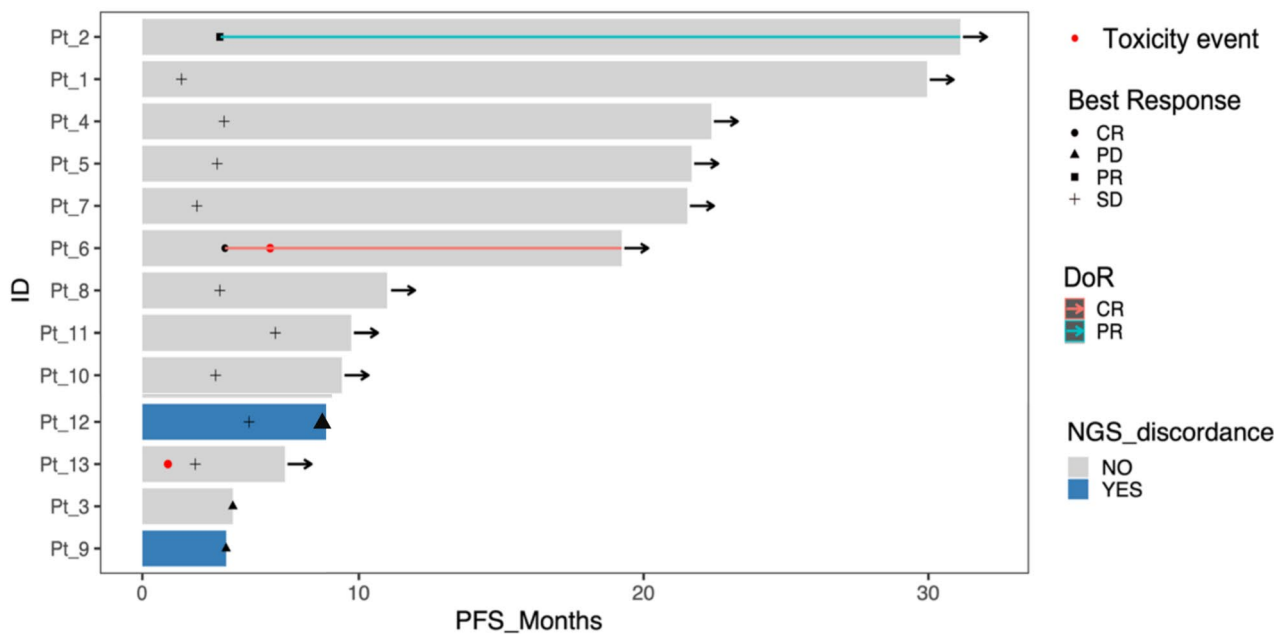


Fig. 6 Swimmer plot for colorectal cancer (CRC) cases. Red dots indicate the event of toxicity, red and cyan arrows indicate the duration of response (DoR). In particular, red arrows for a complete

response (CR) and cyan arrows for a partial response (PR). NGS next-generation sequencing, PD disease progression, PFS progression free survival, Pt patient, SD stable disease

compared with the concordant subgroup ($p > 0.001$ and $p > 0.01$, respectively). In detail, five had *POLE* hotspot mutations, ten had *MSH6* protein loss, eight had atypical MMR deficiency patterns, and six had a MMR germline variant. *POLE* mutations are prevalent in the prognostic characterization of patients with EC. Secondary somatic MMR mutations, often G>T transversions in an aspartyl-glucosaminidase (AGA) gene context, are typically linked to the ultra-mutated phenotype observed in these cases. This can impact MSI or MMR detection, leading to inconsistent test results [44]. Unusual dMMR phenotypes are reported as more prevalent in non-CRC cases (particularly in EC) and frequently associated with genetic syndromes (44.9% vs 21.4% in classical dMMR) [45].

MSH6 protein loss is known to frequently result in correlate with an MSS profile even in PCR-MSI, as *MSH3* can interact with *MSH2* to correct DNA mismatch errors [28, 46]. Specifically, *MSH6* deficiency has been shown to generate ‘minimal microsatellite shifts’ or attenuated MSI signals that fall below standard detection thresholds in NGS and PCR assays [27, 30, 47]. Finally, data provide further evidence that patients with Lynch syndrome, particularly those with *MSH6* mutations, may generally exhibit lower MSI signals than sporadic cases [48].

In contrast, no explanation was found in nearly 60% of discordant cases. However, the presence of *MLH1*

hypermethylation (19 patients) and germline or somatic variants (ten patients) in 29 patients, support MMR findings suggesting that MSI calls may have been missed. Lowering the MSI threshold to 6.1 reduced the number of discordant EC cases to 31. However, to rule out the influence of center-specific factors, external validation is required.

Overall, our findings highlight the limitations of MSI-NGS in EC, consistent with previous observations for MSI-PCR when compared with MMR-IHC. As large genomic panels that also report MSI status are increasingly adopted, caution is warranted when interpreting MSI results, particularly because commonly used thresholds were primarily derived from more prevalent tumor types.

The main limitations of our study include its monocentric design, which may limit the generalizability of the findings and the applicability of the optimized cut-off, the absence of a third confirmatory method such as PCR-MSI considering IHC known limitations, such as its inability to assess the functional activity of expressed proteins and its susceptibility to pre-analytical artifacts and inter-observer variability, particularly in cases of subclonal or weak *MSH6* loss and fixation-related issues, the limited number of microsatellite loci included in the comprehensive genomic profiling panel, of which approximately 49% (62 of 127) were unlikely to be informative for MSI assessment, the tumor-only approach, which precludes evaluation of microsatellite repeat length

shifts that could improve MSI accuracy, and the lack of a long-term follow-up for prognostic correlation. Moreover, the limited number of patients with EC receiving ICI-based treatment prevented us from assessing whether MSI-NGS could identify dMMR patients who do not respond to therapy, as we observed in CRC cases.

The strengths of our study are the large patient cohort and the availability of MLH1 hypermethylation and germline/somatic evaluations, which corroborate the results in some discordant cases. Further analyses on the impact of concurrent somatic mutations and the pattern of unstable loci in concordant and discordant cases, especially comparing EC to CRC, are underway.

5 Conclusions

These findings demonstrate a lower concordance between MMR-IHC and MSI-NGS in EC versus CRC, consistent with available data on MMR-IHC and MSI-PCR. Although optimization of the MSI cut-off improved agreement, the available evidence remains insufficient for clinical implementation, and further validation studies are required. Overall, our results underscore the critical importance of tumor-specific interpretation when applying tumor-agnostic assays, which are often calibrated on more prevalent tumor types. While NGS panels are widely promoted for precision medicine, diagnostic strategies must account for biological differences across cancers.

Supplementary Information The online version contains supplementary material available at <https://doi.org/10.1007/s11523-026-01197-1>.

Acknowledgments Ministry of Health, Ricerca Corrente 2025 MoH, Rc2025.

Authors' contributions CN, LS, SD, GA, and LM contributed to the study design, data interpretation, literature search, and writing of the manuscript. IM, GC, and GT contributed to the data collection. KM, GM, and LG contributed to the data analysis and generation of figures. AM and GM contributed to the genomic analysis; AS and AP contributed to the pathological analysis. AP, MAC, VI, VS, NN, FF, GS, and GT contributed to the revision of the manuscript. All authors read and approved the final paper.

Funding Open access funding provided by Università Cattolica del Sacro Cuore within the CRUI-CARE Agreement. This study was partially funded by the Italian Ministry of Health (Ricerca Corrente; no grant number provided).

Declarations

Conflict of interest Camilla Nero has received travel support from MSD, Illumina, Menarini, and AstraZeneca, and honoraria from Veeva, GSK, MSD, AstraZeneca, Altems, Illumina, and Guardant Health. Lisa Salvatore has served as a consultant or advisor for Am-

gen, AstraZeneca, Bristol-Myers Squibb, Daiichi-Sankyo, Incyte, Lilly, Merck Serono, MSD, and Servier. She has also received research funding from Amgen, Astellas, AstraZeneca, Bayer, BMS, Daiichi-Sankyo, Hutchinson, Incyte, Merck Serono, Mirati, MSD, Pfizer, and Roche. She is part of the speakers' bureaus of Amgen, Bristol-Myers Squibb, GlaxoSmithKline, Lilly, Merck Serono, Pierre Fabre, Roche, and Servier. Maria Alessandra Calegari has received travel and hospitality support from Pierre Fabre, Amgen, Merck, Servier, and Bayer. He also participates in the advisory board of Merck. Vanda Salutari has received honoraria or consultation fees from Immunogen, MSD, GSK, Menarini, and Steam Line, and participated in company-sponsored speaker's bureaus for MSD, AstraZeneca, GSK, and EISA. Nicola Normanno declares receiving speaker's fees and/or participating in advisory boards for MSD, Bayer, Biocartis, Illumina, Incyte, Roche, BMS, Merck, Thermo Fisher, AstraZeneca, and Eli Lilly. He also received financial support for research projects (institutional grants) from Merck, Thermo Fisher, QIAGEN, Roche, AstraZeneca, Biocartis, and Illumina. He has non-financial interests as the President of the International Quality Network for Pathology (IQN Path) and as the Past President of the Italian Cancer Society (SIC). Francesco Fanfani has received research funding from Clovis, GSK, MSD, and PharmaMar, as well as personal and financial interests with GSK, MSD, SYSMEX, and STRYKER. Giovanni Scambia has received research support from MSD and honoraria from Clovis Oncology, and serves as a consultant for Tesaro and Johnson & Johnson. Giovanni Trovato has participated in advisory boards and sponsored meetings organized by BMS, MSD, Merck, AstraZeneca, Pfizer, Servier, Roche, and Dompé. Simona Duranti, Gloria Anderson, Luca Mastrantonio, Mina Karimi, Giulia Mantini, Angelo Minucci, Giulia Maneri, Luciano Giacò, Angela Santoro, Arianna Panfili, Alessia Piermattei, Ilenia Marino, Giulia Caira, Giovanni Trovato, and Valentina Iacobelli have no conflicts of interest that are directly relevant to the content of this article.

Ethics approval The study has been conducted following the Declaration of Helsinki and has received approval from the Fondazione Policlinico Universitario "A. Gemelli" IRCCS ethical committee (Protocol U 00194/23, ID number: 3837).

Consent to participate Prior to participation, all patients provided informed consent.

Consent for publication Not applicable.

Availability of data and material The datasets generated and analyzed during the current study are not publicly available because of ethical reasons, but are available from the corresponding author on reasonable request.

Code availability Not applicable

Open Access This article is licensed under a Creative Commons Attribution-NonCommercial 4.0 International License, which permits any non-commercial use, sharing, adaptation, distribution and reproduction in any medium or format, as long as you give appropriate credit to the original author(s) and the source, provide a link to the Creative Commons licence, and indicate if changes were made. The images or other third party material in this article are included in the article's Creative Commons licence, unless indicated otherwise in a credit line to the material. If material is not included in the article's Creative Commons licence and your intended use is not permitted by statutory regulation or exceeds the permitted use, you will need to obtain permission directly from the copyright holder. To view a copy of this licence, visit <http://creativecommons.org/licenses/by-nc/4.0/>.


References

1. Olave MC, Graham RP. Mismatch repair deficiency: the what, how and why it is important. *Genes Chromosomes Cancer*. 2022;61(3):314–21. <https://doi.org/10.1002/gcc.23015>.
2. Veigl ML, Kasturi L, Olechnowicz J, Ma AH, Lutterbaugh JD, Periyasamy S, et al. Biallelic inactivation of hMLH1 by epigenetic gene silencing, a novel mechanism causing human MSI cancers. *Proc Natl Acad Sci USA*. 1998;95(15):8698–702. <https://doi.org/10.1073/pnas.95.15.8698>.
3. Vilar E, Gruber SB. Microsatellite instability in colorectal cancer: the stable evidence. *Nat Rev Clin Oncol*. 2010;7(3):153–62. <https://doi.org/10.1038/nrclinonc.2009.237>.
4. Hampel H, Frankel WL, Martin E, Arnold M, Khanduja K, Kuebler P, et al. Screening for the Lynch syndrome (hereditary non-polyposis colorectal cancer). *N Engl J Med*. 2005;352(18):1851–60. <https://doi.org/10.1056/NEJMoa043146>.
5. Parsons MT, Buchanan DD, Thompson B, Young JP, Spurdle AB, Hopper JL, et al. Correlation of tumour BRAF mutations and MLH1 methylation with germline mismatch repair (MMR) gene mutation status: a literature review assessing utility of tumour features for MMR variant classification. *J Med Genet*. 2012;49(3):151–7. <https://doi.org/10.1136/jmedgenet-2011-100714>.
6. Ryan NAJ, Glaire MA, Blake D, Cabrera-Dandy M, Evans DG, Crosbie EJ. The proportion of endometrial cancers associated with Lynch syndrome: a systematic review of the literature and meta-analysis. *Genet Med*. 2019;21(10):2167–80. <https://doi.org/10.1038/s41436-019-0536-8>.
7. Cancer Genome Atlas Research Network, Kandoth C, Schultz N, Cherniack AD, Akbani R, Liu Y, et al. Integrated genomic characterization of endometrial carcinoma. *Nature*. 2013;497(7447):67–73. <https://doi.org/10.1038/nature12113>.
8. Cancer Genome Atlas Network, Network TCGA, Kandoth C, Schultz N, Cherniack AD, Akbani R, et al. Comprehensive molecular characterization of human colon and rectal cancer. *Nature*. 2012;487(7407):330–7. <https://doi.org/10.1038/nature11252>.
9. Wang Y, Shi C, Li X, Zhang Q, Chen J, Liu H, et al. Predicting prognosis and immunotherapy response in multiple cancers based on the association of PANoptosis-related genes with tumor heterogeneity. *Genes (Basel)*. 2023;14(11):1994. <https://doi.org/10.3390/genes14111994>.
10. Li K, Zhang L, Wang Y, Chen X, Liu H, Zhao J, et al. Microsatellite instability: a review of what the oncologist should know. *Cancer Cell Int*. 2020;20:16. <https://doi.org/10.1186/s12935-019-1091-8>.
11. Sepulveda AR, Hamilton SR, Allegra CJ, Grody WW, Cushman-Vokoun AM, Funkhouser WK, et al. Molecular biomarkers for the evaluation of colorectal cancer: guideline from the American Society for Clinical Pathology, College of American Pathologists, Association for Molecular Pathology, and the American Society of Clinical Oncology. *J Clin Oncol*. 2017;35(13):1453–86. <https://doi.org/10.1200/JCO.2016.71.9807>.
12. Sargent DJ, Marsoni S, Thibodeau SN, Labianca R, Hamilton SR, French AJ, et al. Defective mismatch repair as a predictive marker for lack of efficacy of fluorouracil-based adjuvant therapy in colon cancer. *J Clin Oncol*. 2010;28(19):3219–26. <https://doi.org/10.1200/JCO.2009.27.1825>.
13. Diaz LA, Shiu KK, Kim TW, Jensen BV, Jensen LH, Punt C, et al. Pembrolizumab versus chemotherapy for microsatellite instability-high or mismatch repair-deficient metastatic colorectal cancer (KEYNOTE-177): final analysis of a randomised, open-label, phase 3 study. *Lancet Oncol*. 2022;23(5):659–70. [https://doi.org/10.1016/S1470-2045\(22\)00197-8](https://doi.org/10.1016/S1470-2045(22)00197-8).
14. European Society of Gynaecological Oncology (ESGO). ESGO-ESTRO-ESP cervical cancer guidelines. Published May 1, 2023. <https://guidelines.esgo.org>. Accessed 31 Jan 2026.
15. Merck Sharp & Dohme LLC. Study of pembrolizumab (MK-3475) in participants with advanced solid tumors (KEYNOTE-158). *ClinicalTrials.gov* identifier: NCT02628067. Published December 17, 2015. Updated May 16, 2023. Available from: <https://clinicaltrials.gov/study/NCT02628067>. Accessed 5 Sept 2024.
16. GlaxoSmithKline. Study to evaluate the efficacy and safety of dostarlimab in combination with carboplatin-paclitaxel in participants with recurrent or primary advanced endometrial cancer (RUBY). *ClinicalTrials.gov* identifier: NCT03981796. Published June 11, 2019. Updated May 7, 2024. <https://clinicaltrials.gov/study/NCT03981796>. Accessed 5 Sept 2024.
17. GlaxoSmithKline. Study of dostarlimab (TSR-042) in participants with recurrent or advanced solid tumors (GARNET). *ClinicalTrials.gov* identifier: NCT02715284. Published March 14, 2016. Updated August 1, 2023. <https://clinicaltrials.gov/study/NCT02715284>. Accessed 5 Sept 2024.
18. Merck Sharp & Dohme LLC. Lenvatinib in combination with pembrolizumab in advanced endometrial cancer (Study 309/KEYNOTE-775). *ClinicalTrials.gov* identifier: NCT03517449. Published May 7, 2018. Updated July 25, 2023. <https://clinicaltrials.gov/study/NCT03517449>. Accessed 5 Sept 2024.
19. Oaknin A, Colombo N, Creutzberg C, Gressel GM, Harter P, Joly F, et al. Endometrial cancer: ESMO clinical practice guideline for diagnosis, treatment and follow-up. *Ann Oncol*. 2022;33(8):860–77. <https://doi.org/10.1016/j.annonc.2022.05.009>.
20. Ferguson J, Grothey A, Kerr D, Thibodeau S, Goldberg RM, Sargent DJ, et al. Immunohistochemistry (IHC) for MMR proteins: a reliable method for identifying mismatch repair deficiency in colorectal cancers. *J Clin Oncol*. 2014;32(1):33–45.
21. Luchini C, Bibeau F, Ligtenberg MJL, Bosse T, Miller K, La Rosa S, et al. ESMO recommendations on microsatellite instability testing for immunotherapy in cancer, and its relationship with PD-1/PD-L1 expression and tumour mutational burden: a systematic review-based approach. *Ann Oncol*. 2019;30(8):1232–43. <https://doi.org/10.1093/annonc/mdz116>.
22. Ryan NAJ, McMahon R, Tobi S, Snowsill T, Evans DG, Crosbie EJ, et al. The proportion of endometrial tumours associated with Lynch syndrome (PETALS): a prospective cross-sectional study. *PLoS Med*. 2020;17(9):e1003263. <https://doi.org/10.1371/journal.pmed.1003263>.
23. Chao X, Li L, Wu M, Wang Y, Zhang Q, Liu H, et al. Comparison of screening strategies for Lynch syndrome in patients with newly diagnosed endometrial cancer: a prospective cohort study in China. *Cancer Commun (Lond)*. 2019;39(1):42. <https://doi.org/10.1186/s40880-019-0388-2>.
24. Ukkola I, Nummela P, Pasanen A, Peltomäki P, Aaltonen LA, Vahteristo P, et al. Detection of microsatellite instability with Idylla MSI assay in colorectal and endometrial cancer. *Virchows Arch*. 2021;479(3):471–9. <https://doi.org/10.1007/s00428-021-03082-w>.
25. Siemanowski J, Schömig-Markieffka B, Buhl T, Stöhr R, Schauer S, Krüger S, et al. Managing difficulties of microsatellite instability testing in endometrial cancer: limitations and advantages of four different PCR-based approaches. *Cancers (Basel)*. 2021;13(6):1268. <https://doi.org/10.3390/cancers13061268>.
26. Gilson P, Levy J, Rouyer M, Demange J, Husson M, Bonnet C, et al. Evaluation of 3 molecular-based assays for microsatellite instability detection in formalin-fixed tissues of patients with endometrial and

- colorectal cancers. *Sci Rep.* 2020;10(1):16386. <https://doi.org/10.1038/s41598-020-73421-5>.
27. Sowter P, Maxwell P, Quek RGW, Speirs V, McVeigh T, Schömig-Markiefka B, et al. Detection of mismatch repair deficiency in endometrial cancer using the Newcastle MSI assay: concordance with IHC and significance of MSH6 status. *Cancers (Basel)*. 2024;16(23):3970. <https://doi.org/10.3390/cancers16233970>.
 28. Riedinger CJ, Esnakula A, Haight PJ, Suarez AA, Chen W, Gillespie J, et al. Characterization of mismatch-repair/microsatellite instability-discordant endometrial cancers. *Cancer*. 2024;130(3):385–99. <https://doi.org/10.1002/cncr.35030>.
 29. Wang Y, Shi C, Eisenberg R, Vnencak-Jones CL. Differences in microsatellite instability profiles between endometrioid and colorectal cancers: a potential cause for false-negative results? *J Mol Diagn*. 2017;19(1):57–64. <https://doi.org/10.1016/j.jmoldx.2016.07.008>.
 30. Wu X, Snir O, Rottmann D, Wong S, Buza N, Hui P. Minimal microsatellite shift in microsatellite instability high endometrial cancer: a significant pitfall in diagnostic interpretation. *Mod Pathol*. 2019;32(5):650–8. <https://doi.org/10.1038/s41379-018-0179-3>.
 31. Hause RJ, Pritchard CC, Shendure J, Salipante SJ, Niu B, Mardis ER, et al. Classification and characterization of microsatellite instability across 18 cancer types. *Nat Med*. 2016;22(11):1342–50. <https://doi.org/10.1038/nm.4191>.
 32. Zhu L, et al. A novel and reliable method to detect microsatellite instability in colorectal cancer by next-generation sequencing. *J Mol Diagn*. 2018;20(2):225–31. <https://doi.org/10.1016/j.jmoldx.2017.11.007>.
 33. Addante F, et al. Mismatch repair deficiency as a predictive and prognostic biomarker in endometrial cancer: a review on immunohistochemistry staining patterns and clinical implications. *Int J Mol Sci*. 2024;25(3):1056. <https://doi.org/10.3390/ijms25021056>.
 34. Nero C, et al. Further refining 2020 ESGO/ESTRO/ESP molecular risk classes in patients with early-stage endometrial cancer: a propensity score-matched analysis. *Cancer*. 2022;128(15):2898–907. <https://doi.org/10.1002/cncr.34331>.
 35. Nero C, et al. Integrating a comprehensive cancer genome profiling into clinical practice: a blueprint in an Italian referral center. *J Pers Med*. 2022;12(6):1746. <https://doi.org/10.3390/jpm12101746>.
 36. Illumina, Inc. TruSight Oncology 500: tumor mutational burden (TMB) analysis. Published 2018. <https://www.illumina.com/content/dam/illumina-marketing/documents/products/appnotes/trusight-oncology-500-tmb-analysis-1170-2018-009.pdf>. Accessed 5 Sept 2024.
 37. Alexandrov LB, et al. The repertoire of mutational signatures in human cancer. *Nature*. 2020;578(7793):94–101. <https://doi.org/10.1038/s41586-020-1943-3>.
 38. Gu Z, et al. Complex heatmaps reveal patterns and correlations in multidimensional genomic data. *Bioinformatics*. 2016;32(18):2847–9. <https://doi.org/10.1093/bioinformatics/btw313>.
 39. Gu Z, et al. Circlize implements and enhances circular visualization in R. *Bioinformatics*. 2014;30(19):2811–2. <https://doi.org/10.1093/bioinformatics/btu393>.
 40. Mayakonda A, et al. Maftools: efficient and comprehensive analysis of somatic variants in cancer. *Genome Res*. 2018;28(12):1747–56. <https://doi.org/10.1101/gr.239244.118>.
 41. Wickham H. *ggplot2: elegant graphics for data analysis*. New York: Springer; 2016.
 42. Dedeurwaerdere F, et al. Comparison of microsatellite instability detection by immunohistochemistry and molecular techniques in colorectal and endometrial cancer. *Sci Rep*. 2021;11:12880. <https://doi.org/10.1038/s41598-021-91974-x>.
 43. Kang SY, et al. Comparative analysis of microsatellite instability by next-generation sequencing, MSI PCR and MMR immunohistochemistry in 1942 solid cancers. *Pathol Res Pract*. 2022;233:153874. <https://doi.org/10.1016/j.prp.2022.153874>.
 44. Stelloo E, et al. Practical guidance for mismatch repair-deficiency testing in endometrial cancer. *Ann Oncol*. 2017;28(1):96–102. <https://doi.org/10.1093/annonc/mdw542>.
 45. Jaffrelot M, et al. An unusual phenotype occurs in 15% of mismatch repair-deficient tumors and is associated with non-colorectal cancers and genetic syndromes. *Mod Pathol*. 2022;35(5):427–37. <https://doi.org/10.1038/s41379-021-00918-3>.
 46. Pečina-Šlaus N, et al. Mismatch repair pathway, genome stability and cancer. *Front Mol Biosci*. 2020;7:122. <https://doi.org/10.3389/fmolb.2020.00122>.
 47. Wang C, Feng M, Kou Y, Kuang W, Wang W, Liang D. Evaluation of microsatellite instability patterns in mismatch repair deficiency: a retrospective analysis of 285 endometrial cancers. *Front Immunol*. 2025;16:1628979. <https://doi.org/10.3389/fimmu.2025.1628979>.
 48. Helderman NC, Strobel F, Bohaumilitzky L, Terlou D, van der Werf-t Lam AS, van Wezel T, et al. Lower degree of microsatellite instability in colorectal carcinomas from MSH6-associated Lynch syndrome patients. *Mod Pathol*. 2025;38(7):100757. <https://doi.org/10.1016/j.modpat.2025.100757>.

Publisher's Note Springer Nature remains neutral with regard to jurisdictional claims in published maps and institutional affiliations.

Authors and Affiliations

Camilla Nero^{1,2} · Lisa Salvatore^{2,3} · Simona Duranti⁴ · Gloria Anderson^{1,2}  · Luca Mastrantoni² · Mina Karimi⁵ · Giulia Mantini⁵ · Angelo Minucci⁶ · Giulia Maneri⁶ · Luciano Giacobbe⁵ · Angela Santoro⁷ · Arianna Panfili⁴ · Alessia Piermattei⁷ · Ilenia Marino⁴ · Giulia Caira³ · Maria Alessandra Calegari³ · Giovanni Trovato³ · Valentina Iacobelli^{1,2} · Vanda Salutari¹ · Nicola Normanno⁸ · Francesco Fanfani^{1,2} · Giovanni Scambia^{1,2} · Giampaolo Tortora^{2,3}

✉ Gloria Anderson
gloria.anderson@guest.policlinicogemelli.it

¹ Ginecologia Oncologica, Dipartimento di Scienze della Salute della Donna e del Bambino, Fondazione Policlinico Universitario Agostino Gemelli IRCCS, Rome, Italy

² Università Cattolica del Sacro Cuore, Rome, Italy

³ Oncologia Medica, Comprehensive Cancer Center, Fondazione Policlinico Universitario Agostino Gemelli IRCCS, Rome, Italy

⁴ Direzione Scientifica, Fondazione Policlinico Universitario Agostino Gemelli IRCCS, L.go A. Gemelli 8, 00168 Rome, Italy

- ⁵ Bioinformatics Core Facility, Gemelli Science and Technology Park (G-STeP), Fondazione Policlinico Universitario Agostino Gemelli IRCCS, Rome, Italy
- ⁶ Departmental Unit of Molecular and Genomic Diagnostics, Genomics Core Facility, Gemelli Science and Technology Park (G-STeP), Fondazione Policlinico Universitario Agostino Gemelli IRCCS, Rome, Italy
- ⁷ UOC Anatomia Patologica, Dipartimento Scienze di Laboratorio ed Ematologiche, Fondazione Policlinico Universitario Agostino Gemelli IRCCS, Rome, Italy
- ⁸ Istituto Romagnolo per lo Studio dei Tumori “Dino Amadori”-IRST IRCCS, Meldola, FC, Italy